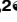



RESEARCH ARTICLE

E-cadherin bridges cell polarity and spindle orientation to ensure prostate epithelial integrity and prevent carcinogenesis *in vivo*

Xue Wang^{1,2}, Baijun Dong³, Kai Zhang², Zhongzhong Ji², Chaping Cheng², Huifang Zhao², Yaru Sheng², Xiaoxia Li², Liancheng Fan³, Wei Xue³, Wei-Qiang Gao^{1,2*}, Helen He Zhu^{1,3*}

1 State Key Laboratory of Oncogenes and Related Genes, Renji-Med-X Stem Cell Research Center, Ren Ji Hospital, School of Medicine, Shanghai Jiao Tong University, Shanghai, China, **2** School of Biomedical Engineering & Med-X Research Institute, Shanghai Jiao Tong University, Shanghai, China, **3** Department of Urology, Renji Hospital, School of Medicine, Shanghai Jiao Tong University, Shanghai, China

 These authors contributed equally to this work.

* gao.weiqiang@sjtu.edu.cn (W-QG); zhuhecrane@shsmu.edu.cn (HHZ)



 OPEN ACCESS

Citation: Wang X, Dong B, Zhang K, Ji Z, Cheng C, Zhao H, et al. (2018) E-cadherin bridges cell polarity and spindle orientation to ensure prostate epithelial integrity and prevent carcinogenesis *in vivo*. PLoS Genet 14(8): e1007609. <https://doi.org/10.1371/journal.pgen.1007609>

Editor: Gregory S. Barsh, Stanford University School of Medicine, UNITED STATES

Received: March 10, 2018

Accepted: August 2, 2018

Published: August 17, 2018

Copyright: © 2018 Wang et al. This is an open access article distributed under the terms of the [Creative Commons Attribution License](https://creativecommons.org/licenses/by/4.0/), which permits unrestricted use, distribution, and reproduction in any medium, provided the original author and source are credited.

Data Availability Statement: The RNA-seq raw data in this paper are available at the GEO (accession number GSE115204). All other relevant data are within the paper and its Supporting Information files.

Funding: The study is supported by funds from the Chinese Ministry of Science and Technology (2017YFA0102900, 2013CB945600), the National Natural Science Foundation of China (NSFC, 81630073 and 81372189), Science and Technology Commission of Shanghai Municipality

Abstract

Cell polarity and correct mitotic spindle positioning are essential for the maintenance of a proper prostate epithelial architecture, and disruption of the two biological features occurs at early stages in prostate tumorigenesis. However, whether and how these two epithelial attributes are connected *in vivo* is largely unknown. We herein report that conditional genetic deletion of E-cadherin, a key component of adherens junctions, in a mouse model results in loss of prostate luminal cell polarity and randomization of spindle orientations. Critically, E-cadherin ablation causes prostatic hyperplasia which progresses to invasive adenocarcinoma. Mechanistically, E-cadherin and the spindle positioning determinant LGN interacts with the PDZ domain of cell polarity protein SCRIB and form a ternary protein complex to bridge cell polarity and cell division orientation. These findings provide a novel mechanism by which E-cadherin acts an anchor to maintain prostate epithelial integrity and to prevent carcinogenesis *in vivo*.

Author summary

Luminal cells are the most abundant type of the prostate epithelial cells. Most prostate cancers also display a luminal phenotype. Horizontal cell division of luminal cells allows the surface expansion of the secretory prostate lumen and meanwhile maintains the monolayer and polarized epithelial architecture. Disruption of the epithelial integrity and appearance of multilayer epithelia are early events in prostate adenocarcinoma development. However, the molecular mechanism that ensures the horizontal division in luminal cells remains largely unknown. Here, we generated a genetically engineered mouse model in which E-cadherin, a key component of the adherens junction that serves to connect the lateral plasma membrane of neighboring epithelial cells, was knocked out in the prostate luminal cells. E-cadherin deletion leads to loss of cell polarity and disoriented cell division,

(16JC1405700), KC Wong foundation, and SJTU-USYD seed funding for Joint Research to W-QG, NSFC (81772743), the State Key Laboratory of Oncogenes and Related Genes (90-16-03), Shanghai Institutions of Higher Learning (The Program for Professor of Special Appointment (Young Eastern Scholar, QD2015002)), School of Medicine, Shanghai Jiao Tong University (Excellent Youth Scholar Initiation Grant 16XJ11003), Ren Ji Hospital (Seed Project RJZZ14-010) to HHZ. The funders had no role in study design, data collection and analysis, decision to publish, or preparation of the manuscript.

Competing interests: The authors have declared that no competing interests exist.

which subsequently causes dysregulated cell proliferation and strongly predisposes mice for prostate tumorigenesis. Importantly, we revealed that E-cadherin acts as an anchor to recruit cell polarity protein SCRIB and spindle positioning determinant LGN to the lateral cell membrane, thereby ensure a proper alignment of the cell division plane. All these findings uncover a novel mechanism by which E-cadherin links cell polarity and spindle orientation to keep prostate epithelial integrity and prevent carcinogenesis.

Introduction

The prostate initially arises from embryonic urogenital sinus and undertakes ductal morphogenesis postnatally [1,2]. Murine prostatic epithelia are comprised of an inner single layer of polarized luminal cells, an outer layer of loosely distributed basal cells and a small fraction of scattered neuroendocrine cells [3,4]. Basal and luminal cells in the developing prostate epithelium display distinct cell division modes [5]. Luminal cells undergo symmetrical cell divisions during which the spindle orientation aligns parallel to the epithelial lumen and mother cell divides horizontally to generate two luminal cells. In contrast, basal cells undergo either horizontal symmetrical cell divisions to reproduce themselves or vertical asymmetrical cell divisions to give rise to a basal and a luminal daughter cell [5]. Horizontal cell division is of great importance for not only the surface expansion of prostate secreting lumen but also the maintenance of a monolayer luminal epithelial architecture, loss of which is an early event in prostate adenocarcinoma development. However, the molecular mechanism that ensures the horizontal symmetrical cell division of prostate luminal cells remains largely unknown.

Previous work has demonstrated that cell polarity is indispensable for correct cell division orientations. Cell polarity are instructed by three types of asymmetrically distributed polarity protein complexes, the Scribble (SCRIB)/Lethal giant larvae (LGL)/Discs large (DLG) protein complex beneath the basolateral cell membrane, the partitioning defective 3 (PAR3)/PAR6/atypical protein kinase (aPKC) in the cell apical-basal domain, and the Crumbs/PALS/PATJ protein complex under the apical cell membrane. Intensive studies in *Drosophila* have demonstrated that distribution cues for the spindle orientation determinants are derived from cell polarity [6]. An evolutionally conserved leucine-glycine-asparagine repeat protein (LGN)/nuclear and mitotic apparatus (NUMA)/inhibitory alpha subunit of heterotrimeric G protein (G α i) complex, which forms a lateral cortical belt to generate forces on spindle astral microtubules through interacting with dynein/dynactin, has been shown to be a major spindle positioning machinery [7]. Apical distribution of polarity protein aPKC phosphorylates LGN to exclude LGN from the apical cortex and determines the planar plane of the cell division [8–11]. DLG can interact directly with LGN and control its localization to orient the spindle position [12–14]. SCRIB or DLG knockdown in the developing *Drosophila* wing disc epithelium results in spindle orientation defects [15]. Nevertheless, how the polarity cues and horizontal spindle orientation are connected in mammalian systems is not fully understood.

Adherens junctions are closely associated with cell polarity and mitotic spindle positioning. They provide spatial landmarks for the anchorage of polarity proteins such as SCRIB and DLG [16]. Disrupted adherens junctions due to low calcium lead to diffused cell polarity protein localization in mammalian epithelial cells [17]. In neuroepithelial cells of *Drosophila*, adherens junction defects cause a shift of cell division modes due to deviation of spindle positioning from the planar axis and uncoupling of spindle positioning from asymmetric basal protein localization [18]. In the *Drosophila* follicular epithelium, adherens junctions prompt the apical position of the midbody to achieve asymmetric cytokinesis [19]. While these studies implicate

the importance of adherens junctions in cell polarity and spindle positioning, the evidence for adherens junction proteins, such as E-cadherin, as a bridge between the two events is lacking. Importantly, expression of E-cadherin is frequently lost or downregulated in human prostate cancers [20–22]. Whether and how the loss of E-cadherin leads to prostate tumorigenesis remain poorly understood.

In the present study, using a murine prostate-specific E-cadherin knockout model, we find that E-cadherin connects the cell polarity and spindle positioning to ensure the horizontal symmetric division of luminal cells and the integrity of prostate epithelia. Importantly, we show that a cell polarity protein SCRIB is recruited by E-cadherin to form an E-cadherin/SCRIB/LGN complex to guarantee the proper cell division mode and to prevent prostatic carcinogenesis.

Results

Loss of E-cadherin leads to a hyperproliferative phenotype of prostatic luminal cells and development of prostate adenocarcinoma in aged mice

To unravel the role of adherens junctions in prostate epithelial development and homeostasis, we first examined expression patterns of E-cadherin, a key component of adherens junctions, at different developmental stages via triple staining for E-cadherin, the basal prostatic cell-specific marker p63 and the luminal cell marker CK8. We found that E-cadherin was expressed throughout the epithelium at postnatal day 5 (P5), and then more predominantly expressed in the lateral cell membrane of tightly-contacted prostatic luminal cells than scattered basal cells over time (S1 Fig). Using the Cre-LoxP recombination system, we generated a mouse model in which E-cadherin was specifically knocked out in the prostate epithelium by crossing *Cdh1^{fl/fl}* mice with probasin-cre transgenic mice. Immunostaining results confirmed an efficient E-cadherin deletion in the prostate of *Pcre;Cdh1^{fl/fl}* mice (Fig 1A and 1B). Through immunofluorescent staining of Ki67, a mitotic cell marker, we observed a significant increase of proliferative luminal cells from different lobes of *Pcre;Cdh1^{fl/fl}* mice at P5, P10 and P15 or during adult prostate regeneration, compared with their littermate controls (Fig 1C and 1D, S2A and S2B Fig and S1 Table). In contrast, significantly elevated cell proliferation was only detected in p63⁺ cells from P5 but not P10 or P15 *Pcre;Cdh1^{fl/fl}* mouse prostates (Fig 1C and 1D, S2A and S2B Fig and S1 Table). This is possibly due to the minimal expression of E-cadherin in basal cells at P10 and P15. Those data suggest that E-cadherin deficiency leads to a hyperproliferative phenotype of prostatic luminal cells.

To determine whether this hyperproliferation led to prostate cancer initiation, we carefully followed prostates of *Pcre;Cdh1^{fl/fl}* mice and their control littermates from 6 weeks to 21 months postnatally. Immunohistochemical staining analysis showed that at 6 weeks, different prostate lobes (anterior, ventral and dorsolateral lobes) of *Pcre;Cdh1^{fl/fl}* mice developed multifocal epithelial hyperplasia and multilayered polyp-like structure (S2C Fig). We detected low-grade murine intraepithelial neoplasia (mPIN) in 4 months old *Pcre;Cdh1^{fl/fl}* mice (Fig 2A). By 9 months of age, *Pcre;Cdh1^{fl/fl}* mice developed high-grade mPIN, characterized by increased number of atypical cells with nuclear enlargement, prominent nucleoli and an elevated nuclear to cytoplasmic ratio (Fig 2B). As shown in Fig 2B–2D and S2 Table, more than 60% of 9-month-old and 80% 21-month-old E-cadherin deficient prostatic lumens exhibited a hyperplastic phenotype. Of note, we detected invasive adenocarcinoma in the prostates from 37.5% of 21-month-old *Pcre;Cdh1^{fl/fl}* mice manifested by loss of p63⁺ basal cells, disruption of the basement membrane, as demonstrated by loss of laminin staining and invasion of epithelial cells into the surrounding prostatic stroma (Fig 2E–2G).

We further conducted RNA sequencing on prostates from E-cadherin knockout and control animals. Genes regulating cellular biological processes including cell proliferation, cell

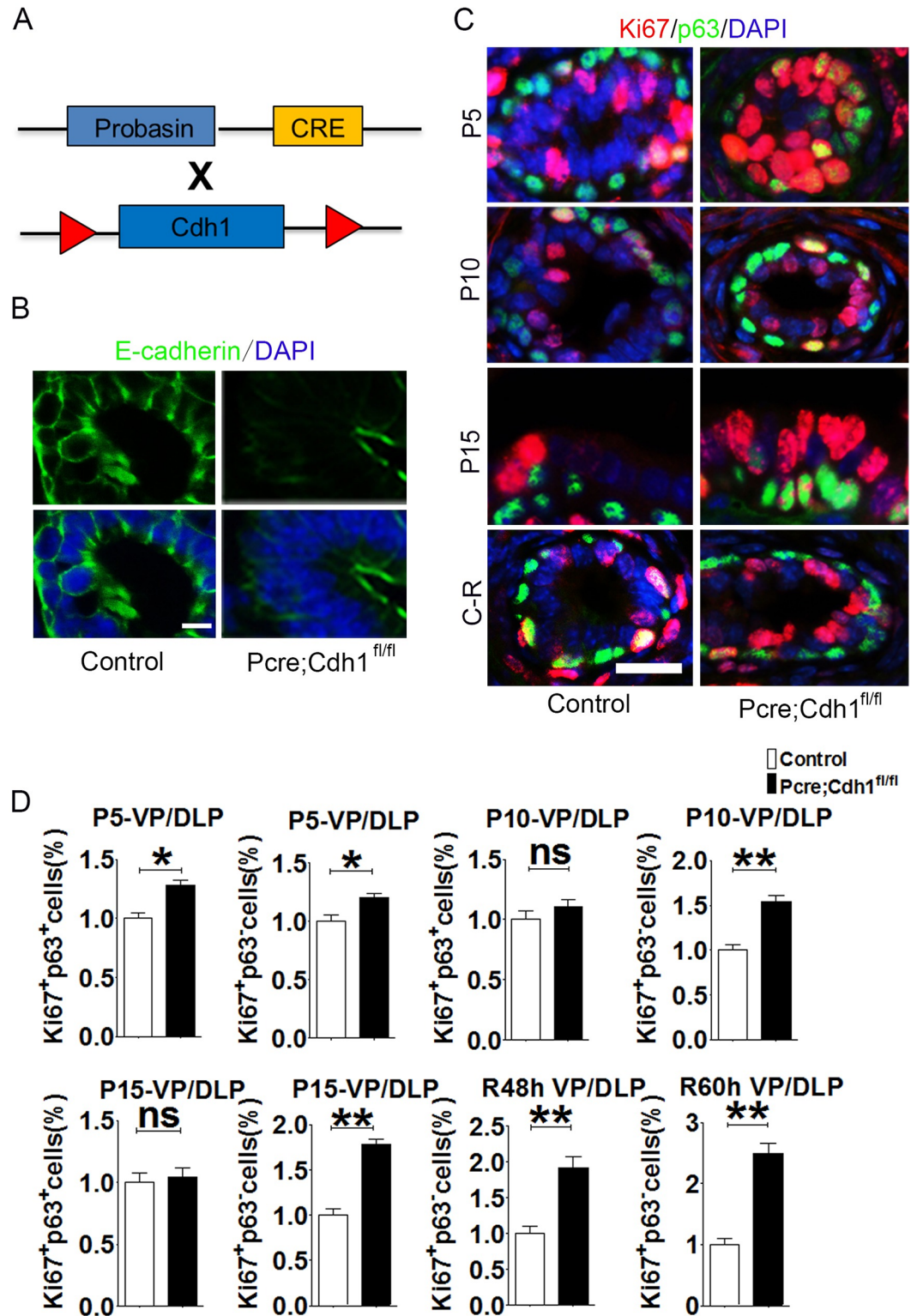


Fig 1. E-cadherin ablation leads to a hyperproliferative phenotype of prostatic luminal cells. (A) The schematic illustrates the generation of a mouse model with prostatic specific knockout of E-cadherin. (B) The efficiency of conditional E-cadherin deletion is confirmed by immunofluorescent staining. (C) Analysis of cell proliferation in developing prostates (P5, P10 and P15) or regenerating prostates (48h and 60h after androgen replacement) by immunofluorescent co-staining of proliferative marker Ki67 and basal cells marker p63 (Scale bars are 20µm for (B) and (C)). (D) Quantification of mitotic

epithelial cells from ventral and dorsolateral prostatic lobes at different development stages or regeneration time points (n = 3, Student's *t*-test, ***P<0.001, **P<0.01, *P<0.05, error bars = SEM.).

<https://doi.org/10.1371/journal.pgen.1007609.g001>

adhesion and cell migration were the most transcriptionally altered genes (S3 Fig and S3 Table). We performed additional qRT-PCR confirmation experiments. As shown in S3D Fig, genes which act to promote cell proliferation and cell migration were more preferentially expressed in the E-cadherin null prostate epithelial cells, whereas molecules that facilitate cell junctions were significantly downregulated in E-cadherin knockout prostate epithelia. Moreover, we utilized the TCGA human prostate cancer database to compare the transcriptional signature between our E-cadherin knockout mouse model and human prostate cancer (S4 Fig). As shown in S4 Fig, we found that the transcriptional profile of E-cadherin knockout mouse prostates resembled the human prostate cancer. This data further substantiated the relevance of E-cadherin knockout mice as a valuable prostate cancer model. Together, those data provided additional molecular explanations to the hyperproliferative phenotype and invasive adenocarcinoma detected in E-cadherin knockout prostates.

Further immunofluorescent staining confirmed the E-cadherin deletion in actively proliferating prostate epithelial cells from *Pcre;Cdh1^{fl/fl}* mice. The vast majority of tumor cells in aged *Pcre;Cdh1^{fl/fl}* prostates also displayed an absence of E-cadherin expression, indicating that the tumors were derived from hyperproliferation of E-cadherin knockout cells (Fig 3A and 3B). However, E-cadherin deletion did not result in an epithelial to mesenchymal transition, as we did not observe an enhanced expression of mesenchymal cell marker vimentin in *Pcre;Cdh1^{fl/fl}* prostate epithelial cells (Fig 3C). Similar to human prostate cancer samples, we also occasionally detected apoptotic epithelial cells in *Pcre;Cdh1^{fl/fl}* mouse prostate tumors (Fig 3D).

Horizontal division of prostate luminal cells is randomized by E-cadherin deletion during postnatal development and regeneration

Previous studies have shown that planar spindle alignment in epithelia is crucial for the maintenance of mitotic daughter cells within the plane of the tissue, whereas spindle orientation perpendicular to the basement membrane is required for asymmetric cell divisions and epithelial stratification in tissues such as skin [23]. The expansion of a monolayer developing prostate lumen is ensured by the horizontal division of luminal cells [5], disruption of which often causes multilayered polyps-like structure as detected in *Pcre;Cdh1^{fl/fl}* prostates. We therefore wondered whether loss of E-cadherin affected proper spindle alignment of dividing luminal cells during postnatal prostate development. To test this possibility, we analyzed the spindle orientation of dividing luminal cells by staining sections of developing prostates with p63 and survivin, an approach used for analysis of cell division modes [5]. We observed a more than 2-fold increase of tilted and vertical cell divisions in luminal cells in P5 E-cadherin knockout prostates (40.0% in *Pcre;Cdh1^{fl/fl}* mice versus 14.2% in control mice). Similar findings were obtained from P10 and P15 prostates (Fig 4A, 4C and 4D and S4 Table). In addition, during adult prostate regeneration, E-cadherin deletion resulted in randomization of the luminal cell division plane (Fig 4B and 4E and S4 Table). Collectively, these findings suggest that E-cadherin is required for a proper mitotic spindle orientation during prostate development and regeneration.

Interference of E-cadherin expression results in spindle dis-orientation in the prostatic RWPE-1 cell line

To directly test whether E-cadherin loss led to defects in spindle positioning and subsequently cell division orientation, we modified a previously reported approach to record the spindle

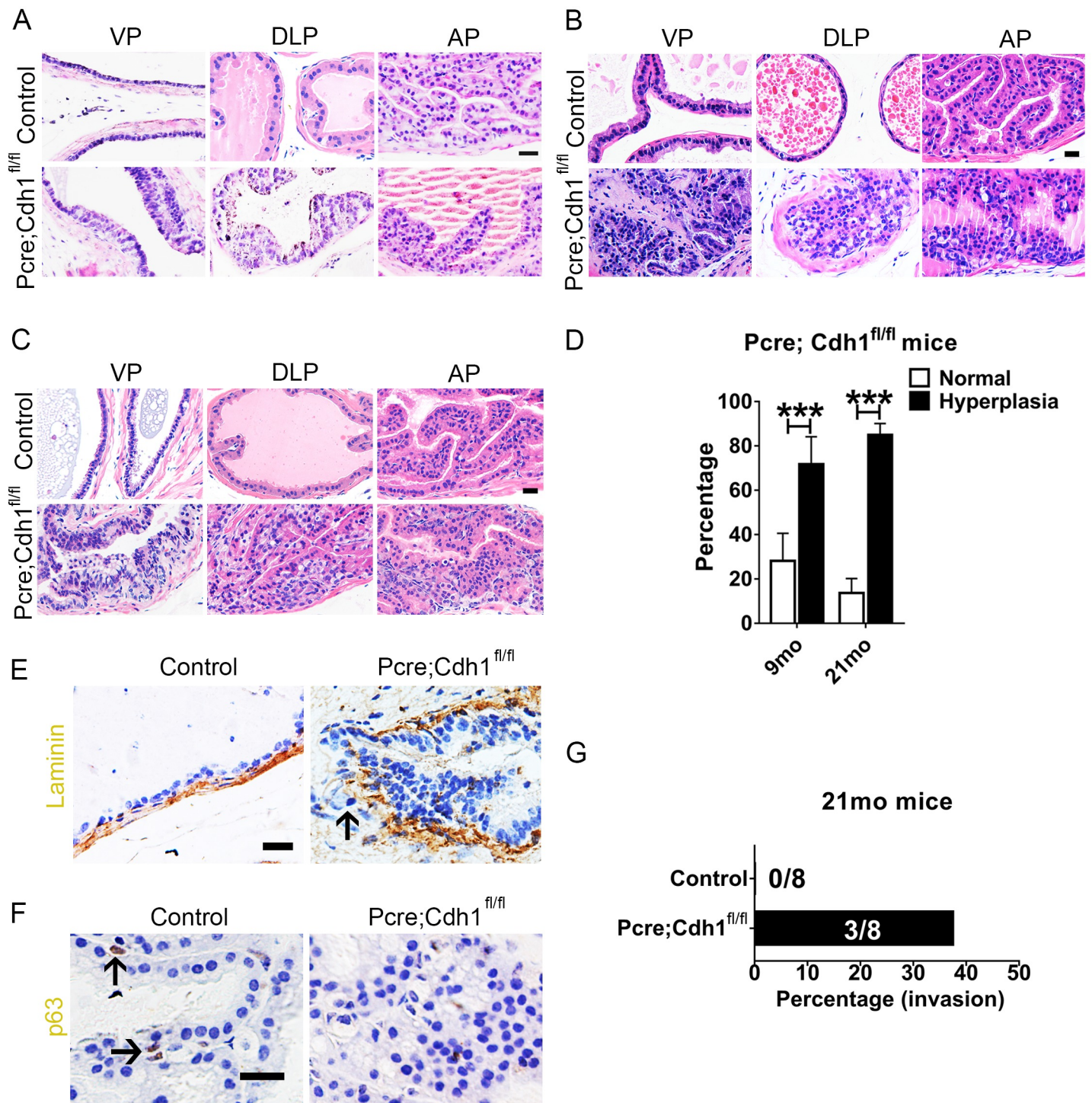


Fig 2. E-cadherin knockout results in development of invasive prostate adenocarcinoma. (A) H&E staining shows that multilayered epithelia structure and hyperplastic lesions can be found in 4-month old E-cadherin knockout mouse prostates. (n = 4) (B) Nine-month old E-cadherin knockout mouse prostates develop high-grade murine intraepithelial neoplasia. (control n = 5, *Pcre;Cdh1^{fl/fl}* n = 6) (C) H&E staining shows adenocarcinoma in the prostates of 21-month-old *Pcre;Cdh1^{fl/fl}* mice. (n = 8) (D) Quantification of hyperplastic lumens in total prostate lumens from 9- or 21-month-old mice. (E) Immunohistochemistry staining of laminin indicates the disruption of the basement membrane and invasion of epithelial cells into the surrounding prostatic stroma in adenocarcinoma from *Pcre;Cdh1^{fl/fl}* prostates. (F) Loss of p63⁺ basal cells in adenocarcinoma from *Pcre;Cdh1^{fl/fl}* prostates (Scale bars are 20µm). (G) Quantification of the invasive incidence from 21-month-old mice. (Student's *t*-test, ***P*<0.01, **P*<0.05, error bars = SEM. 9 month, control n = 5, *Pcre;Cdh1^{fl/fl}* n = 6; 21 month, n = 8).

<https://doi.org/10.1371/journal.pgen.1007609.g002>

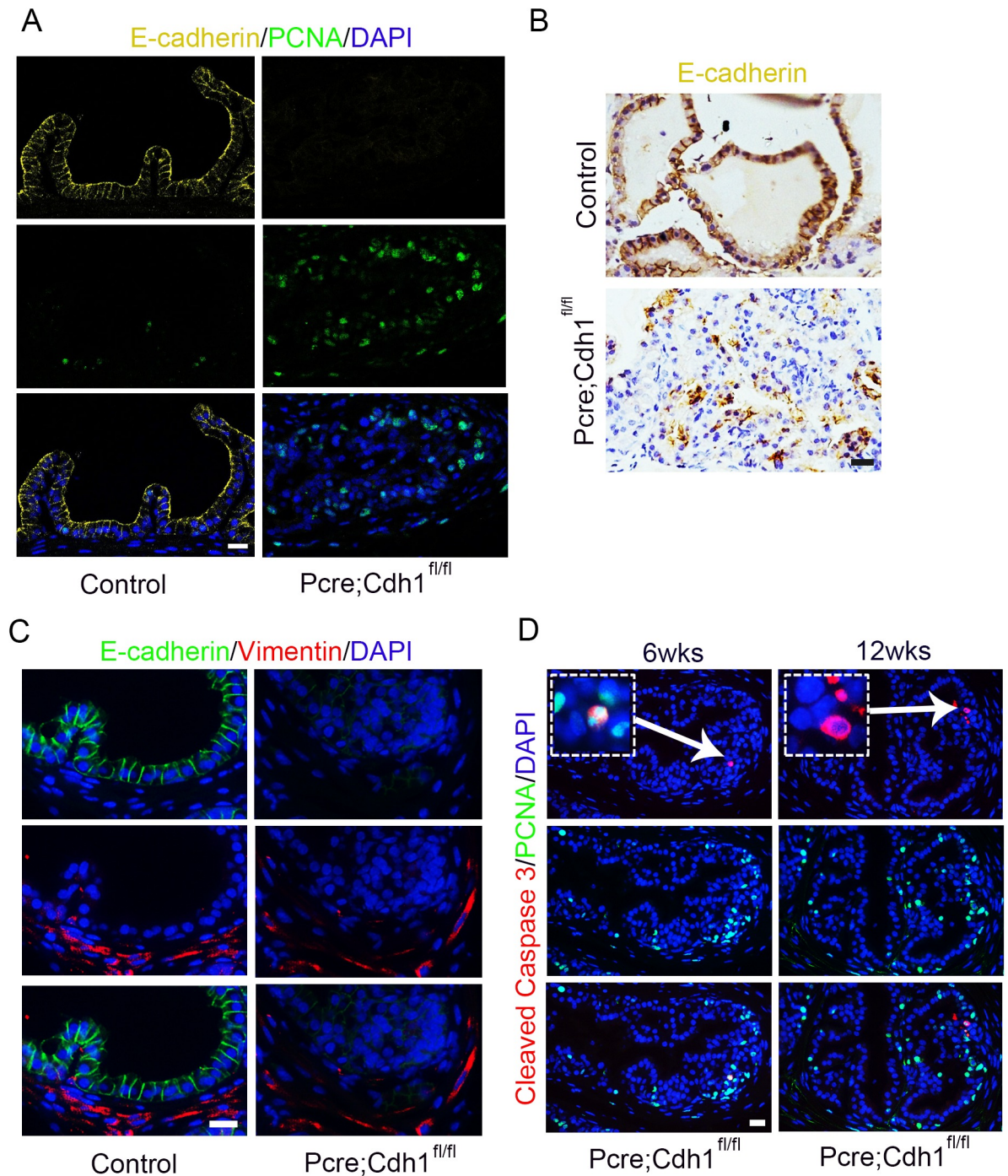


Fig 3. Tumors in *Pcre;Cdh1^{fl/fl}* prostates are derived from hyperproliferation of E-cadherin knockout cells. (A) IF staining confirms E-cadherin deletion in actively proliferating prostate epithelial cells of E-cadherin knockout mice. (B) Tumor cells in aged E-cadherin knockout prostates display absence of E-cadherin expression. (C) E-cadherin ablation does not result in an epithelial to mesenchymal transition (EMT). (D) Apoptotic epithelial cells are occasionally detected in hyperproliferative multilayered regions of E-cadherin knockout mouse prostates (Scale bars are 20µm).

<https://doi.org/10.1371/journal.pgen.1007609.g003>

position of an immortalized prostate epithelial cell line RWPE-1 in real time [24,25]. RWPE-1 cells were co-transfected with an H2B-RFP and an α -tubulin-GFP plasmid to mark chromosomes and spindles respectively (Fig 5A). Knockdown of E-cadherin was achieved by infection

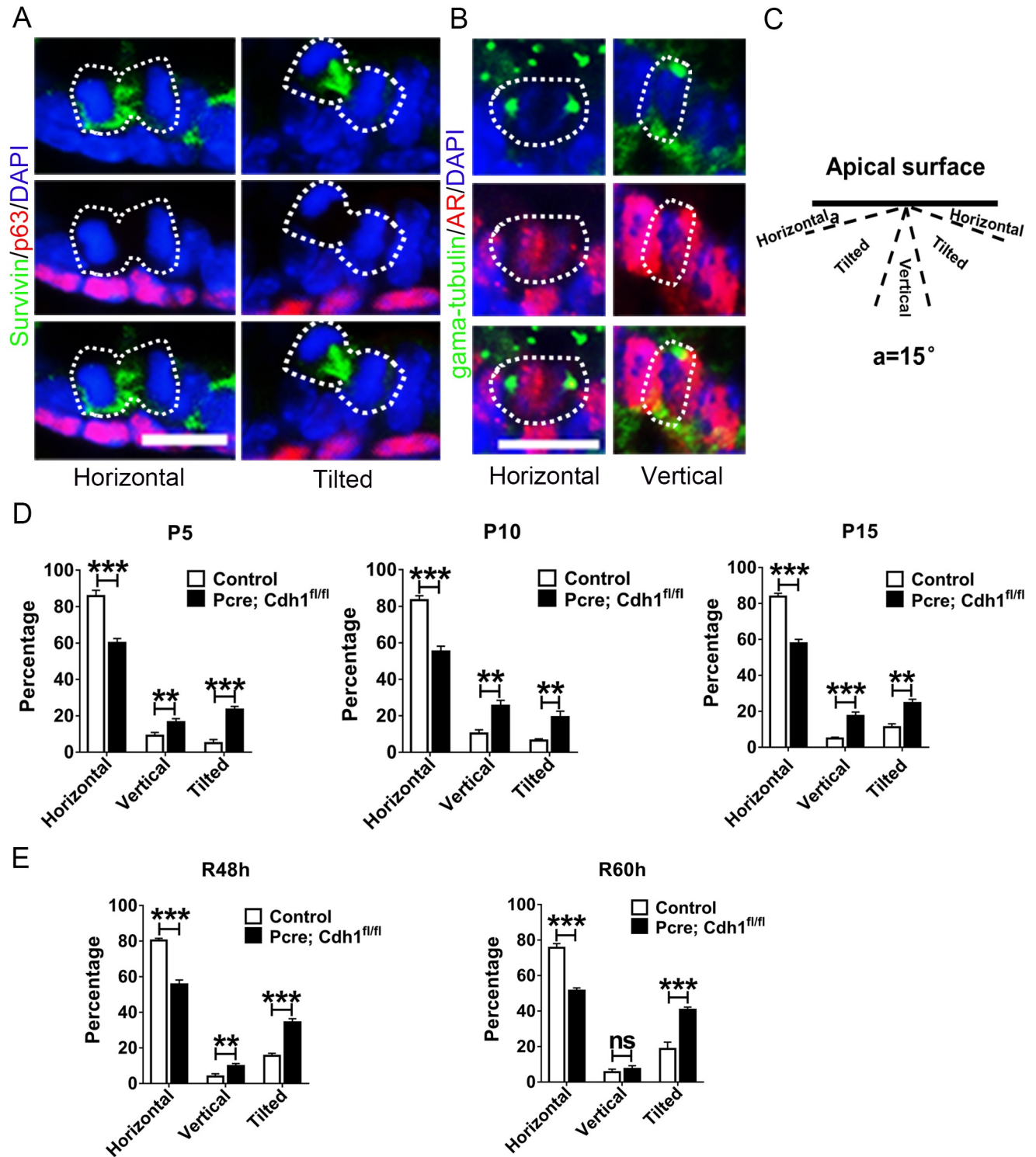


Fig 4. Oriented cell division of prostate epithelial cells during postnatal development and regeneration is randomized by E-cadherin deletion *in vivo*. (A) Immunofluorescent staining of p63, survivin and DAPI illustrates mitotic spindle orientation of dividing prostate epithelial cells. (B) Co-staining of AR, gamma-tubulin and DAPI shows that prostate luminal cells mostly undergo horizontal divisions and very rarely go through vertical divisions during prostate development (Scale bars are 10µm for A and B). (C) The schematic in the left panel depicts the definition of horizontal, tilted or vertical spindle orientation based on the angles of spindle alignment relative to the apical surface. Division planes positioned at 75–90 degrees relative to the basement membrane were defined as vertical divisions, those that were oriented at 15–75 degrees were classified as tilted divisions, while those that were oriented at 0–15 degrees were considered as horizontal divisions. (D–E) E-cadherin deletion leads to a significant increase in vertically or obliquely dividing luminal cells during prostate development (D) or regeneration (E).

<https://doi.org/10.1371/journal.pgen.1007609.g004>

of RWPE-1 cells with a shRNA containing lentiviral construct (Fig 5B). Consistent with the *in vivo* E-cadherin knockout data, we detected a higher proliferating rate in E-cadherin knockdown RWPE-1 cells compared to control cells (S5 Fig). Control or E-cadherin knockdown cells were plated on retronectin-coated dishes and imaged under a confocal microscopy equipped with a live-cell recording unit (Fig 5C). Four-dimensional movies of dividing RWPE-1 cells were analyzed to measure angles of mitotic spindles relative to the culture dish. In line with previous reports [26,27], we found that mitotic spindles of control RWPE-1 cells were positioned at a wide range of angles during prometaphase, but the majority of spindles (83.5%) exhibited a parallel orientation to the substrate from the late metaphase to telophase (Fig 5D and 5E, S4 Table and S1 Movie). This horizontal position of spindles ensured a cell division cleavage plane perpendicular to the substrate. However, we detected a striking increased percentage of E-cadherin-knockdown cells which could not correctly position their spindles in telophase, thereby caused a randomized cell division cleavage plane (Fig 5D and 5E, S4 Table and S1 Movie). These *in vitro* experiments substantiated our *in vivo* observations that adherens junction protein E-cadherin was indispensable for the proper positioning of mitotic spindles in prostate epithelial cells.

Ablation of E-cadherin disrupts cellular distribution and association of key spindle positioning proteins LGN and NUMA

Luminal epithelial cells of a developing prostate divide within the plane of the epithelium by orienting spindle poles towards the lateral membrane. Intensive research has revealed that an evolutionarily conserved LGN/NUMA complex plays an essential role in directing the cortical attachment of spindle astral microtubules to dynein in variety tissues from both invertebrates and vertebrates [9,27–29]. In agreement with previous reports, we found that LGN and NUMA formed two crescents underneath the lateral membrane and in parallel to the basal surface in mitotic wild-type prostate luminal cells (Fig 6A–6D). However, in the absence of E-cadherin, distribution of LGN and NUMA in dividing luminal cells can be detected all around the cell cortex (Fig 6A–6D and S5 Table), suggesting that disoriented mitotic spindle alignment was due to the diffused localization of LGN/NUMA complex. In addition, the protein-protein interaction between LGN and NUMA was also severely abrogated after E-cadherin deletion (Fig 6E). As a result, the luminal cells underwent perpendicular or oblique divisions, which disrupted the monolayer epithelial structure and formed the disorganized, multilayered polyps-like structure (Fig 1 and S2 Fig).

Loss of E-cadherin impairs the cell polarity of prostate luminal cells during prostatic development

Cell polarity provides spatial cues to guide spindle orientation [10,12,14,30]. Disruption of cell polarity is often seen during the course of cancer initiation [11,31–35]. Given the observation that horizontal mitotic spindle positioning of prostate luminal cells was severely disrupted in the *Pcre;Cdh1^{fl/fl}* prostate, we therefore wondered whether E-cadherin affected luminal cell polarity. We next investigated the impact of E-cadherin loss on the expression and distribution of PAR complex and SCRIB complex. Utilizing immunofluorescent staining, we detected core components of the PAR complex, PAR3 and aPKC were localized in the apical domain of wild-type prostate luminal cells, but diffusely distributed in *Pcre;Cdh1^{fl/fl}* prostate luminal cells (Fig 6F and 6G and S6A and S6B Fig). Likewise, the normal basolateral distribution of polarity proteins DLG-1 and SCRIB in prostate luminal cells were markedly impaired after E-cadherin deletion (Fig 6H and 6I and S6C and S6D Fig). In addition, the formation of SCRIB/DLG polarity protein complex was disrupted following E-cadherin deletion (S6E Fig).

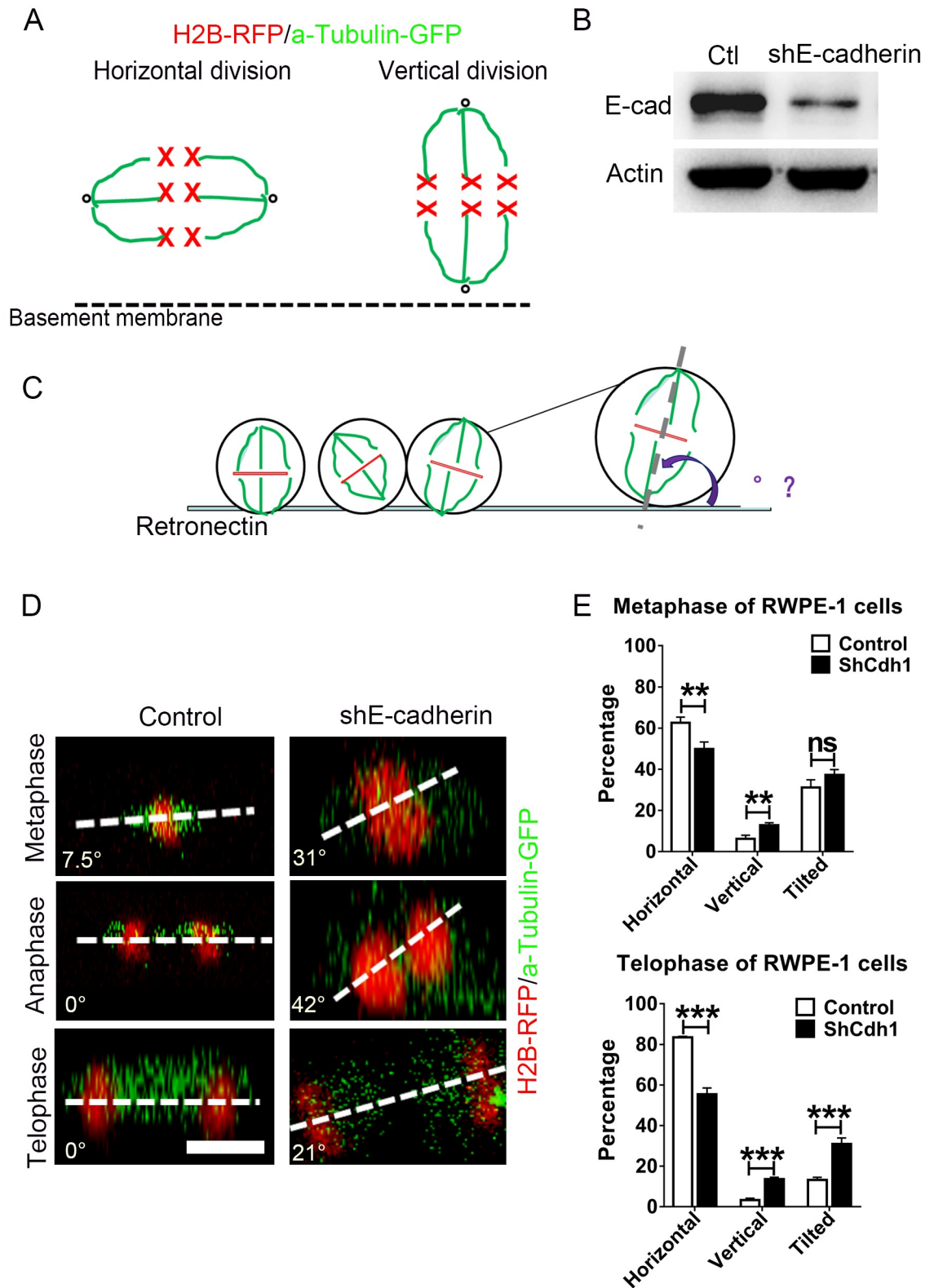


Fig 5. E-cadherin knockdown causes mitotic spindle disorientation in the immortalized prostate cell line RWPE-1. (A) The cartoon illustrates different division modes of epithelial cells. The green lines are α -tubulin-GFP marked spindles and the red crosses depict H2B-RFP labeled chromosomes. (B) The efficiency of E-cadherin knock-down is confirmed by Western blotting. (C) The

cartoon illustrates how the mitotic spindle angle of cultured RWPE-1 cells relative to the retronectin-coated dish bottom is measured. (D) Representative confocal images of α -tubulin-GFP marked spindles and H2B-RFP labeled chromosomes from control or E-cadherin knockdown RWPE-1 cells in different cell cycle phases (Scale bars are 20 μ m). (E) Quantification of metaphase and telophase spindle angles indicated that E-cadherin knockdown causes a remarkable increase of RWPE-1 cells with vertical or oblique mitotic spindle alignment in the telophase.

<https://doi.org/10.1371/journal.pgen.1007609.g005>

Together, these results indicated that loss of E-cadherin exerted a devastating influence on the formation and maintenance of prostate luminal cell polarity.

E-cadherin recruits SCRIB to form an E-cadherin/SCRIB/LGN complex to bridge cell polarity and spindle positioning

Previous research has demonstrated that adherens junctions are necessary for the establishment of cell polarity and positioning mitotic spindles symmetrically in *Drosophila* [18]. Given the aforementioned findings that E-cadherin deletion or knockdown led to cell polarity loss and spindle dis-orientation, we proposed a hypothesis that E-cadherin may serve as a central molecule to bridge cell polarity and spindle positioning. It was reported that in mammalian epithelial cells, restriction of SCRIB to the lateral cell-cell junction is dependent on E-cadherin and that SCRIB reciprocally regulates E-cadherin-mediated cell adhesion [16,36,37]. On the other hand, lateral localization of the SCRIB polarity complex determines the planar orientation of mitotic spindles [14,15,38,39]. Therefore, we then tested whether there were physical interactions between E-cadherin and SCRIB. Co-IP assay showed endogenous interactions between E-cadherin and SCRIB in RWPE-1 cells (Fig 7A and 7B). In addition, we observed that E-cadherin associated with LGN (Fig 7A and 7C). To elucidate whether possible interactions existed between the SCRIB complex and the LGN complex in prostate epithelial cells, we carried out additional co-IP experiments. Intriguingly, we found that endogenous SCRIB interacted with LGN, which can be suppressed by E-cadherin knockdown (Fig 7B and 7D). Furthermore, the association between LGN and E-cadherin was markedly attenuated by SCRIB knockdown (Fig 7E). SCRIB knockdown led to an increase in RWPE1 cell proliferation (S7 Fig). To determine whether the interactions between E-cadherin and SCRIB, as well as LGN with SCRIB were direct, and which domains of SCRIB were responsible for the interactions, we designed and performed GST-pull down experiments with different truncated fragments of SCRIB. As show in Fig 7F and 7G, the fragment containing the PDZ domain of SCRIB directly bound to both the E-cadherin and LGN. Collectively, these data revealed a ternary protein complex of E-cadherin/SCRIB/LGN by which adherens junctions were able to tightly regulate and efficiently connect cell polarity complexes and spindle orientation determinants so to precisely position mitotic spindles in dividing cells (Fig 8).

Discussion

At the current study, we find that genetic deletion of E-cadherin in the mouse prostate results in cell polarity loss, mitotic spindle dis-orientation, and monolayer structure disruption in the luminal epithelium. Importantly, E-cadherin knockout leads to prostatic hyperplasia which progresses to invasive adenocarcinoma in aged mice. Mechanistically, E-cadherin can recruit SCRIB to form a protein complex with LGN by directly binding to the PDZ domain of SCRIB to restrict SCRIB and LGN to the lateral cell membrane. These findings provide a novel mechanism that E-cadherin acts as a vital bridge between cell polarity and spindle orientation for the maintenance of a normal prostate epithelial architecture.

In both *Drosophila* and mammalian systems, adherens junctions, cell polarity and mitotic spindles orientation are intricately intertwined biological processes. However, how these three

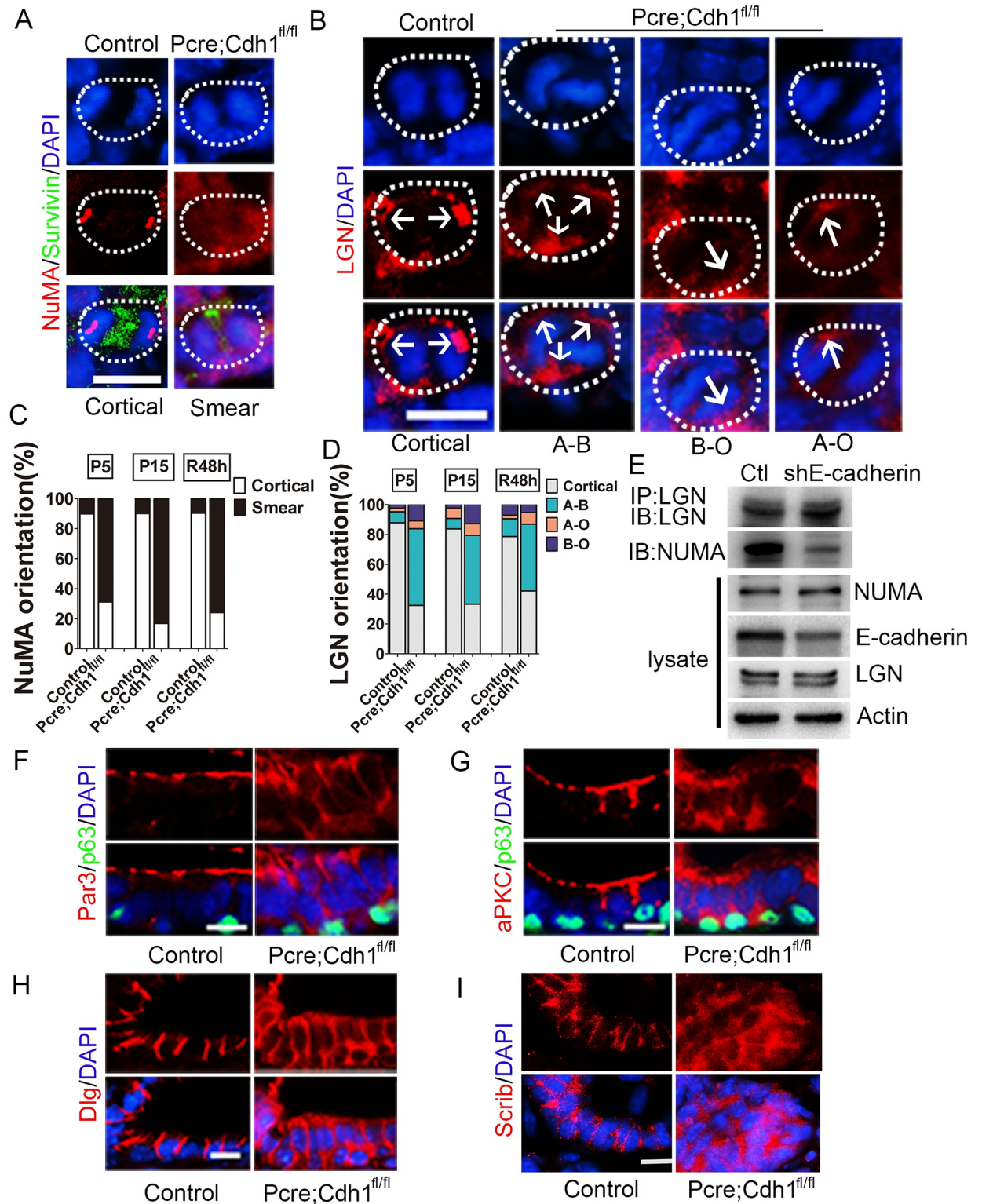


Fig 6. Ablation of E-cadherin disrupts the distribution of key spindle positioning and cell polarity proteins of prostate luminal cells. (A) Immunofluorescent staining of NUMA shows that E-cadherin depletion in the mouse prostate diminishes NUMA cortical enrichment. (B) LGN can be detected all around the cell cortex of dividing E-cadherin knockout prostate epithelial cells, in comparison to its exclusively lateral distribution in wild-type controls. A-B, diffused LGN position; B-O, basal surface enriched LGN position; A-O, apical surface enriched LGN position. (C) Quantification of the NUMA localization pattern in dividing luminal cells during prostate development and regeneration. (D)

Quantification of ratios of each type of LGN distributions in dividing luminal cells during prostate development and regeneration. (E) The formation of LGN/NUMA protein complex is markedly suppressed due to E-cadherin knockdown *in vitro*. (F-G) Wild-type prostate luminal cells exhibit apical distribution of polarity proteins PAR3 (F) and aPKC (G), whereas E-cadherin deleted luminal cells display a diffused expression pattern of those polarity proteins. (H-I) Immunostaining of basolateral polarity proteins, DLG (H) and SCRIB (I) shows that the basolateral polarity of luminal cells is dispersed by E-cadherin ablation. All sections were collected from P15 prostate tissues and counterstained by 4',6-diamidino-2-phenylindole(DAPI)(blue) (Scale bars are 10 μ m).

<https://doi.org/10.1371/journal.pgen.1007609.g006>

fundamental attributes of the epithelium are connected remains elusive. In particular, limited previous studies regarding this question were mostly carried out in cell lines or in invertebrates. The current study was carried out in a genetically engineered mouse model. Our examination of early murine postnatal prostate development and adult regeneration reveals that E-cadherin deletion results in loss of luminal cell polarity and mitotic spindle dis-orientation *in vivo*. In addition, other than microscopic examination of cell mitosis at limited time points, we used a real-time recording system which allows us to follow the whole process of individual cell division. By this way, we further demonstrate vividly that E-cadherin is required for the horizontal alignment of spindles in the telophase of dividing RWPE1 cells *in vitro*. Critically, we uncover a central role of adherens junction protein E-cadherin in the coordination of cell polarity and mitotic spindles orientation by forming an E-cadherin/SCRIB/LGN protein complex. E-cadherin knockout leads to a dis-assembly of the SCRIB polarity complex and the LGN/NUMA complex, causing a subsequent randomization of the luminal cell division plane and forming of multilayered, disorganized epithelia, a common feature of the early stage of prostate tumorigenesis.

During the preparation of our manuscript, Nelson, W.J.'s group reported that, based on biochemical analysis and examination of MDCK and U2OS cell lines, E-cadherin instructs cell division orientation by binding to LGN and brings LGN to cell-cell adhesions, [40]. In a related study on MDCK cells, Hart, K.C. et al reported that E-cadherin acts to sense mechanical tension across an epithelial sheet and facilitate polarized cortical distribution of LGN to align cell divisions[41]. However, whether this LGN/E-cadherin complex is important for epithelial tissue integrity and the consequences of disruption of this interaction *in vivo* is unknown. In addition, whether additional components, such as cell polarity, are required to the intricate regulation of LGN by E-cadherin is not determined. Our current study shed new important lights on these aspects: 1) We demonstrated clearly *in vivo* that E-cadherin knockout causes LGN/NUMA dissociation and dis-localization during luminal cell mitosis, which subsequently leads to luminal cell division plane dis-orientation and serious impairment of normal prostate architecture; 2) We provide direct evidences that cell polarity protein SCRIB is required for the efficient complex-forming between E-cadherin and LGN in prostate epithelial cells, as SCRIB knockdown markedly reduces the association of E-cadherin and LGN. Moreover, we found that both E-cadherin and LGN can directly bind to the fragment containing PDZ domain of SCRIB by pull down assays. Of note, our experiments also provide a novel molecular explanation for previous reports regarding how SCRIB is required for the establishment of E-cadherin-mediated cell-cell adhesion and correct positioning of mitotic spindles [16,36,37].

Defects in precisely controlled cell-cell adhesion and junctions, cell polarity and mitotic spindles position are closely associated with developmental disorders, and may contribute to cancer initiation and progression [34,42,43]. For example, conditional knockout of cell polarity protein SCRIB in mouse prostates has been reported to lead to prostatic intraepithelial neoplasia [44]. This is consistent with our observation that SCRIB knockdown promotes RWPE1 cell proliferation. Decreased expression or genetic loss of adherens junction molecule E-cadherin is frequently found in various cancer types including gastric carcinomas, lung cancer

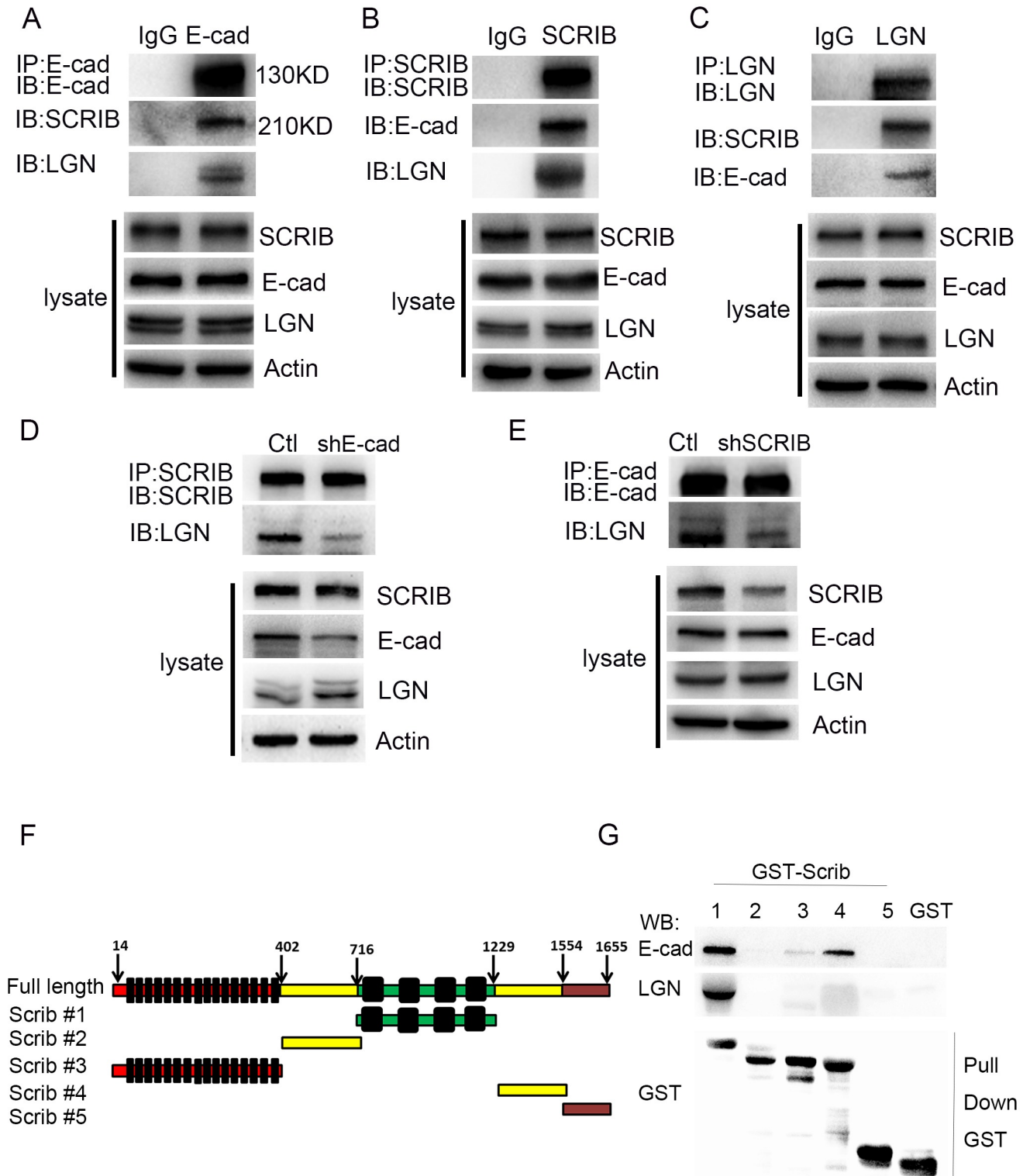


Fig 7. E-cadherin recruits SCRIB to form an E-cadherin/SCRIB/LGN complex to connect cell polarity and spindle positioning. (A) Co-IP experiments using RWPE-1 cell lysates suggest that endogenous E-cadherin interacts with SCRIB and LGN. (B) Endogenous SCRIB co-immunoprecipitates with the E-cadherin/LGN protein complex. (C) Co-IP assays indicate that endogenous SCRIB, E-cadherin and LGN form a ternary complex. (D) The interaction between SCRIB and LGN is suppressed by E-cadherin knockdown. (E) SCRIB knockdown attenuates the association between LGN and E-cadherin. (F) Diagram of SCRIB fragments used to identify E-cadherin and LGN binding domains. (G) Pull down assays indicate the fragment containing PDZ domain of SCRIB binds to E-cadherin and LGN.

<https://doi.org/10.1371/journal.pgen.1007609.g007>

Working model

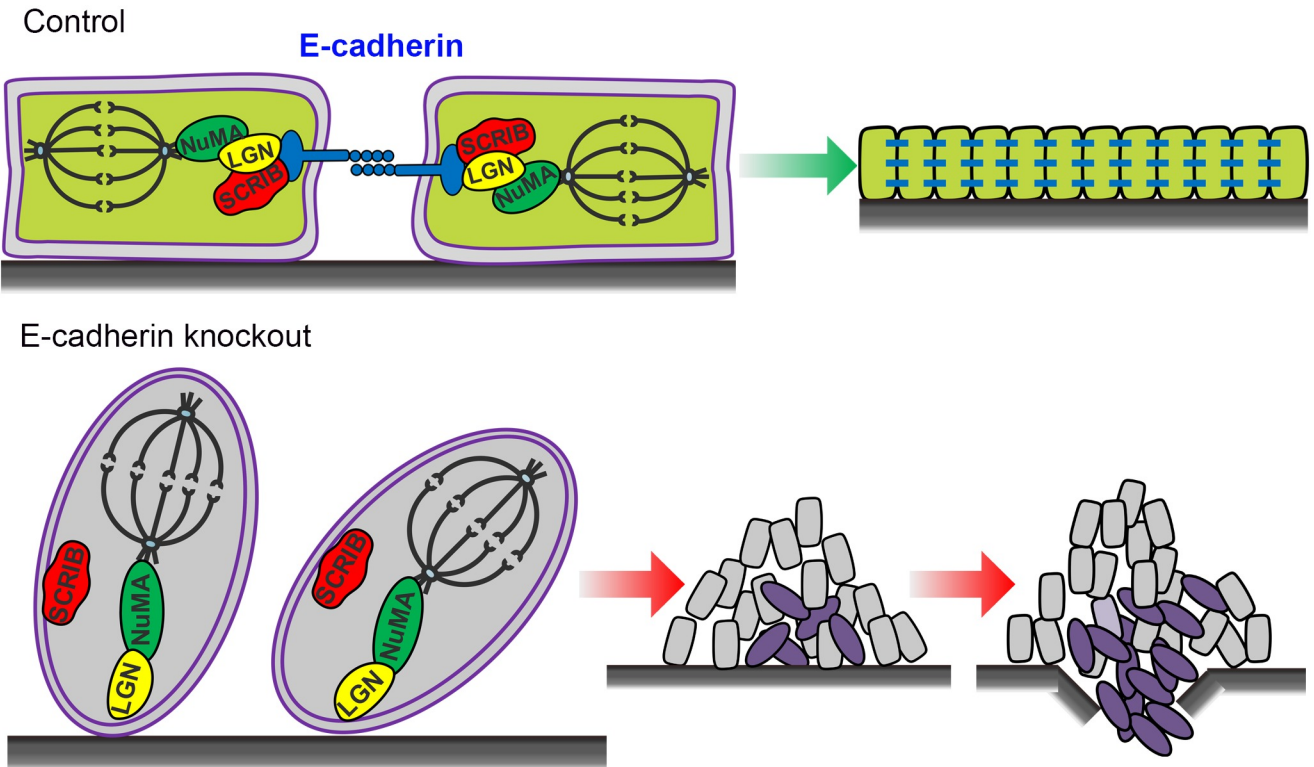


Fig 8. The working model shows adherens junction protein E-cadherin recruits SCRIB to the LGN/NUMA complex to connect the cell polarity and mitotic spindle positioning. E-cadherin loss leads to disruption of prostate luminal cell polarity and randomization of spindle orientations, which strongly predispose mice for prostate tumorigenesis.

<https://doi.org/10.1371/journal.pgen.1007609.g008>

and breast cancer [45–47]. In prostate cancer, E-cadherin down regulation is significantly associated with advanced stages and tumor metastasis [20–22]. A recent study using a *NKX3.1 cre-ERT2;Cdh1^{fl/fl}* mouse model showed that tamoxifen induced partial E-cadherin deletion in luminal cells from 8-week old mice leads to a short-term of anoikis [48]. While we do also detect some apoptotic cells in hyperplastic lumen of *Pcre;Cdh1^{fl/fl}* prostates in this study, we demonstrate that a more efficient prostate epithelium deletion of E-cadherin leads to luminal epithelial cell hyperplasia. Those apoptotic luminal cells may come from actively perpendicular or oblique dividing cells that lose cell-cell contact or cell-basement membrane contact. Apoptotic luminal cells can also be frequently found in human prostate cancer samples. A similar simultaneous increase in both proliferation and apoptosis was reported in PAR3 deletion-induced mammary gland hyperplasia [35]. In addition, our observation that invasive prostate carcinoma develops in old E-cadherin knockout mice is in line with a clinical correlation between E-cadherin deletion or downregulation and human prostate cancer progression [20,21]. Moreover, immunofluorescent staining of developmental prostate or tumor tissues from *Pcre;Cdh1^{fl/fl}* mice confirms E-cadherin deletion in most proliferating luminal cells, suggesting that the hyperplasia is not derived from compensatory proliferation of residue E-cadherin expressing cells. Therefore, loss of E-cadherin induced cell polarity and cell division plane deregulation can strongly predispose mice for prostate tumorigenesis. These findings provide evidence for an important role of E-Cadherin not only in anchorage of cell polarity proteins with spindle positioning determinants, but also in prostatic carcinogenesis.

Methods

Ethics statement

All mice were maintained and utilized according to the ethical regulations at Ren Ji Hospital. The animal protocols were approved by the Ren Ji Hospital Laboratory Animal Use and Care Committee. CO₂ asphyxiation is used for sacrificing mice.

Experimental animals

Probasin-Cre and *Cdh1^{fl/fl}* mice were introduced from National Cancer Institute (NCI:01XF5) and Jackson laboratory (JAX:005319) respectively. Prostates of male mice were dissected for histology and immunostaining.

Human cell Lines

Prostate immortalized epithelial cell line RWPE-1 cells (CRL-11609) were cultured in defined keratinocyte-SFM basic medium with growth supplements (Gibco, 10744–019). Cells were propagated in an incubator with 5% CO₂ at 37°C.

Plasmids and lentivirus production

The shRNA against E-cadherin, SCRIB and scramble shRNA were cloned into a lentiviral vector pLVTH. Lentivirus was produced as previously reported[49]. RWPE-1 cells were infected with lentivirus and selected with 3ug/ml puromycin for 2weeks to generate the stable E-cadherin and SCRIB knockdown cell line, respectively. The H2B-RFP (#26001) and α -tubulin-GFP (#64060) plasmids were purchased from Addgene, which were originally deposited by Dr. Beronja S. and Dr. Yang W.

Castration and androgen replacement

Pcre;Cdh1^{fl/fl} mice and their control littermates were surgically castrated. Three weeks after castration, dihydrotestosterone (MCE, HY-A0120) dissolved in sterile corn oil was given via intraperitoneal injection twice each day (50ug/d) to induce prostate regeneration. Prostate tissues were dissected for section and immunofluorescent staining at different regeneration stages (48 hours or 60 hours post testosterone administration).

Immunofluorescence staining

Mouse prostates were fixed in 4% paraformaldehyde for 20 minutes and dehydrated in 30% sucrose solution overnight. Tissues were then embedded in Optimal Cutting Temperature (O.C.T.) compound and quickly frozen in a -80°C refrigerator for 10min. Frozen sections were cut at a thickness of 6 μ m. The sections were washed with PBS and subjected to a heat-induced epitope retrieval step in 0.01M sodium citrate (PH 6.0). Then sections were transferred to a blocking solution (PBS with 0.2% TritonX-100 and 10% donkey serum) for 1 hour at room temperature. Primary antibodies diluted in PBS with 0.2% TritonX-100 and 1% donkey serum were then applied to the section overnight at 4°C and washed away with PBS three times. Sections were then incubated with secondary antibodies, conjugated to Alexafluor-488, 594 or 546 for 1 hour at room temperature. After thorough washing, sections were mounted with Vector Shield mounting medium containing DAPI.

Immunohistochemical staining

Paraffin-embedded tissue sections were deparaffinized, rehydrated and subjected to a heat-induced epitope retrieval step in 0.01M sodium citrate (PH 6.0). Endogenous peroxidase activity was ablated by using 3% hydrogen peroxide. Sections were blocked, stained with primary antibodies then horseradish peroxidase conjugated secondary antibodies as described above. Then DAB staining was undertaken according to the manufacturer's instructions (DAB Staining kit, GK347010, Gene Tech (Shanghai) Company Limited). Sections were washed under running tapping water for 5min then counterstained with hematoxylin, followed by dehydration and mounting with the neutral balsam mounting medium.

GST-Pull down

Human SCRIB full length was cloned from the cDNA of the RWPE-1 cell line. GST-tagged fragments of human SCRIB were cloned into the pET-49b(+)vector with SpeI and EcoRI restriction enzymes. DNA constructs were transformed into BL21 (DE3) E.coli for following recombinant protein expression. For protein purification, glutathione sepharose beads (GE Healthcare) were added to the recombinant protein containing bacterial lysate and incubated for 1.5 hours at 4°C. Beads were washed with 500µl cold bacteria lysis buffer twice. RWPE-1 cell lysate was added to the beads and incubated overnight at 4°C. After thorough wash, protein loading buffer were added to the beads and boiled for 10 minutes at a 100°C metal bath. The immunoprecipitates were analyzed by SDS-PAGE and immunoblotting with GST, or indicated antibodies.

Immunoprecipitation and immunoblotting

For immunoprecipitation, RWPE-1 cells were washed with ice-cold phosphate-buffer saline and lysed in a lysis buffer (50mM Tris-HCL, 150mM NaCl, 1mM EDTA, 0.25% TritonX-100, PH7.4) supplemented with protease and phosphatase inhibitors (Roche, Penzberg, Germany). Cell lysates were incubated with 1µg primary antibodies for 6 hours at 4°C. Rabbit or mouse immunoglobulin G (Sigma-Alrich, USA) was utilized as controls. Activated Protein G-Agarose (Roche, 11243233001) were added into the protein lysate and incubated for another 1 hour at 4°C. Then the immunoprecipitates were washed 3 times with the lysis buffer and denaturalized for 10 minutes at a 100°C metal bath. The Immunoprecipitation results were detected by immunoblotting assay. Protein samples were separated via SDS-PAGE electrophoresis and then transferred to PVDF membranes. The membranes were blocked with 5% non-fat milk in TBST (TBS containing 0.1% Tween 20) and incubated with primary antibodies at 4°C overnight. Membranes were then rinsed with TBST for 3 times and incubated with secondary antibodies for 1 hour at room temperature. After washing with TBST 3 times, membranes were exposed with enhanced chemiluminescence substrates (Thermo Scientific). Antibodies used in the study were listed in [S6 Table](#).

Confocal microscopy for images and videos

Lentivirus-transfected RWPE-1 cells were seeded on glass-bottom dishes coated with 0.1µg/µl Retronectin (Takara Bio). Images were acquired every 6–7 minute with a xyzt acquisition mode using an Axio Observer under a Z1 microscope with the LSM 700 scanning module (Zeiss). Cell cultures were maintained at 37°C and 5% CO₂ incubator for live imaging.

RNA extraction and quantitative-PCR analysis

To collect single prostate epithelial cells suspension for flow cytometric sorting of basal, luminal and stromal cells, prostates from 12-week-old Pcre;Cdh1fl/fl mice and control littermates

were harvested, minced and incubated with 3ml 1mg/ml Collagenase solution on a shaker at 37°C for 2 hours. The cells were then spin down and further digested with 2ml 0.25% Trypsin/EDTA at a 37°C water-bath for another 6 minutes. Single cells were obtained by filtering the mixture through a 40µm cell strainer. Percp-lineage, FITC-CD49f, APC-Sca-1 antibodies were applied to the cell suspension and incubated in the dark for 40 minutes. Basal (Lineage⁻Sca-1⁺CD49f⁺), luminal epithelial cells (Lineage⁻Sca-1⁻CD49f⁺) and stromal cells (Lineage⁻Sca-1⁺CD49f⁻) were sorted using a BD FACSARIA system. Total RNA were extracted from each cell population using Trizol reagents following instructions from the manufacturer (Life technologies). cDNA was synthesized from the extracted total RNA using PrimeScript RT Reagent Kit (RR037A). qPCR was performed using SYBR Premix Ex Taq (TliRNaseH Plus) (RR420A). Relative transcript abundance was determined by the comparative CT method using Actin as a reference gene. Primers used in RT-PCR were listed in [S7 Table](#).

RNA-seq and data analysis

Single Lineage⁻Epcam⁺PI⁻ prostate epithelial cell suspension from 3-mo old Ecadherin knock-out mice and their control littermates were FACS sorted before processing to total RNA extraction, quality control and library preparation. Libraries were constructed using NEBNext Ultra Directional RNA Library Prep Kit for Illumina (NEB, USA) following manufacturer's recommendations and index codes were added to attribute sequences to each sample. The clustering of the index-coded samples was conducted on a cBot Cluster Generation System using TruSeq PE Cluster Kit v3-cBot-HS (Illumina) according to the manufacturer's recommendations. The libraries were sequenced on an Illumina HiSeq platform and paired-end reads were obtained. The software btrim was utilized to discard low quality reads whose insert size were less than 30, or average quality score within a moving window were less than 20. The clean data were mapped to the Mus musculus reference genome (GRCm38). Gene expression levels and differential expression were analyzed using the Cufflinks and Cuffdiff program, respectively, in the Cufflinks tool suite (v2.2.1) with default parameters. The functional annotation of differentially expressed genes was performed using the database for annotation, visualization and integrated discovery software (DAVID v6.8). The RNA-seq raw data in this paper are available at the GEO web with the accession number GSE115204.

Quantification and statistical analysis

The ImageJ 1.46r software was used to determine the positive stained cells in immunostaining images and measure angles of mitotic spindles relative to the retronectin base. Microsoft Excel and Graph Pad Prism5 were used for data compilation and graphical representation. All bar graphs, line graphs and dot plots are represented as mean ± standard deviation. All statistical analysis was done using a two-tailed Student's *T-test* and a p-value < 0.05 was considered significant and indicated by a star (*) mark.

Supporting information

S1 Fig. E-cadherin is preferentially expressed in prostatic luminal cells. (A) Confocal images showing expression patterns of E-cadherin at indicated developmental stages. Scale bars are 20µm. (B) RT-PCR analysis shows that E-cadherin is predominantly expressed in prostate luminal cells. Luminal, basal and stromal cells from 2-month old mice were enriched using flow cytometric sorting based on lineage, Sca1 and CD49f staining. (n = 3. Data are presented as mean ± s.e.m, and the P value was determined by the Student's t-test, ***P<0.01, **P<0.05) (TIF)

S2 Fig. E-cadherin deletion results in a significantly elevated mitotic activity of luminal cells in prostate development and regeneration. (A) Sections of anterior lobes (AP) of developing or regenerating prostates at indicated time points were stained with the proliferative marker Ki67 and basal cells marker p63. Slides were counterstained by DAPI. (n = 3) (B) Quantification of Ki67 positive cells suggests that E-cadherin knockout leads to hyperproliferation of luminal cells in prostate development and regeneration. (Student's *t*-test, ** $P < 0.01$, * $P < 0.05$, error bars = SEM. n = 3) (C) H&E staining shows that multilayered epithelia structure can be early found in 6-week-old E-cadherin knockout mouse prostates. (Scale bars are 20 μ m. for (A) and (C), n = 3)

(TIF)

S3 Fig. RNA-seq data uncover genes regulating proliferation, adhesion and migration are the most transcriptionally altered genes. (A) Gene Ontology (GO) analysis reveals an enrichment of cell proliferation, migration and cell junctions associated molecules or signaling pathways. (B) A heatmap showing the expression levels for cell proliferation associated genes. (C) A heatmap illustrating the expression levels for cell junctions and cell migration associated genes. (D) qRT-PCR data confirm hyperproliferative and malignant phenotypes in transgenic mice.

(TIF)

S4 Fig. The transcriptional profile of E-cadherin knockout mouse prostates resembled the human prostate cancer. Patterns of E-cadherin-regulated signature genes which were represented in the TCGA database of human prostate cancer expression profiles.

(TIF)

S5 Fig. E-cadherin knockdown upregulates RWPE-1 cell proliferation. Cell number was determined by a Cell Counting Kit 8 assay (n = 5 duplicates).

(TIF)

S6 Fig. Cell polarity is severely impaired in E-cadherin knockout prostate epithelial cells. (A-B) Sections of P5 and adult prostates were stained with antibodies against PAR3 (A), aPKC (B) and p63. Apical distribution of PAR3 or aPKC in luminal cells were disrupted by E-cadherin knockout. (n = 3) (C-D) Immunostaining of P5 and adult prostates shows that normal basolateral localization of polarity proteins DLG-1 (C) and SCRIB (D) become diffused in E-cadherin deleted luminal cells. (All sections are counterstained with DAPI. Scale bars are 10 μ m. n = 3) (E) The formation of DLG/SCRIB protein complex is markedly suppressed due to E-cadherin knockdown in RWPE-1 cells.

(TIF)

S7 Fig. SCRIB knockdown promotes RWPE-1 cell proliferation. Cell number was determined by a Cell Counting Kit 8 assay (n = 5 duplicates).

(TIF)

S1 Table. Quantification of percentage of proliferative epithelial cells in different prostate lobes during postnatal development and regeneration.

(DOCX)

S2 Table. Quantification of percentages of normal, PIN and adenocarcinoma phenotypes of the prostatic histology in 9-mo and 21-mo old Ecadherin knockout mice.

(DOCX)

S3 Table. Differential expressed genes detected in RNA-seq analysis. The highlight section represented the fold change of 324 genes was over 2.

(XLSX)

S4 Table. Quantification of percentages of horizontal, vertical and titled divisions in mitotic epithelial cells at different murine prostate development and regeneration stages, as well as in RWPE-1 cells of different cell cycle phases.

(DOCX)

S5 Table. Quantification of percentages of each type of LGN and NUMA distributions in dividing luminal cells in different prostate development and regeneration stages.

(DOCX)

S6 Table. Antibodies used in this paper.

(DOCX)

S7 Table. Primers used in this paper.

(DOCX)

S1 Movie. The movie dynamically showing the horizontal or titled divisions in mitotic RWPE-1 prostatic epithelial cells. (H2B-RFP and α -tubulin-GFP).

(MP4)

Acknowledgments

Thanks for the assistance from Wei Zhou in the RNA-seq data analysis.

Author Contributions

Conceptualization: Wei-Qiang Gao, Helen He Zhu.

Data curation: Xue Wang, Kai Zhang, Zhongzhong Ji, Chaping Cheng, Yaru Sheng.

Formal analysis: Xue Wang.

Investigation: Xue Wang, Baijun Dong.

Methodology: Xue Wang, Helen He Zhu.

Resources: Baijun Dong, Xiaoxia Li, Liancheng Fan, Wei Xue.

Software: Zhongzhong Ji, Huifang Zhao.

Supervision: Huifang Zhao, Wei-Qiang Gao, Helen He Zhu.

Validation: Chaping Cheng.

Writing – original draft: Xue Wang, Wei-Qiang Gao, Helen He Zhu.

Writing – review & editing: Xue Wang, Baijun Dong, Wei-Qiang Gao, Helen He Zhu.

References

1. Cunha GR (1994) Role of mesenchymal-epithelial interactions in normal and abnormal development of the mammary gland and prostate. *Cancer* 74: 1030–1044. PMID: [8039137](https://pubmed.ncbi.nlm.nih.gov/8039137/)
2. Xin L, Ide H, Kim Y, Dubey P, Witte ON (2003) In vivo regeneration of murine prostate from dissociated cell populations of postnatal epithelia and urogenital sinus mesenchyme. *Proc Natl Acad Sci* 100: 11896–11903. <https://doi.org/10.1073/pnas.1734139100> PMID: [12909713](https://pubmed.ncbi.nlm.nih.gov/12909713/)
3. Abate-Shen C, Shen MM (2000) Molecular genetics of prostate cancer. *Genes Dev* 14: 2410–2434. PMID: [11018010](https://pubmed.ncbi.nlm.nih.gov/11018010/)
4. Xin L (2013) Cells of origin for cancer: an updated view from prostate cancer. *Oncogene* 32: 3655–3663. <https://doi.org/10.1038/onc.2012.541> PMID: [23178496](https://pubmed.ncbi.nlm.nih.gov/23178496/)

5. Wang J, Zhu HH, Chu M, Liu Y, Zhang C, Liu G, Yang X, Yang R, Gao W-Q (2014) Symmetrical and asymmetrical division analysis provides evidence for a hierarchy of prostate epithelial cell lineages. *Nat Commun* 5: 4758. <https://doi.org/10.1038/ncomms5758> PMID: 25163637
6. Knoblich JA (2008) Mechanisms of Asymmetric Stem Cell Division. *Cell* 132: 583–597. <https://doi.org/10.1016/j.cell.2008.02.007> PMID: 18295577
7. Seldin L, Muroyama A, Lechler T (2016) NuMA-microtubule interactions are critical for spindle orientation and the morphogenesis of diverse epidermal structures. *Elife* 5: 1–18.
8. Du Q, Macara IG (2004) Mammalian Pins is a conformational switch that links NuMA to heterotrimeric G proteins. *Cell* 119: 503–516. <https://doi.org/10.1016/j.cell.2004.10.028> PMID: 15537540
9. Zheng Z, Zhu H, Wan Q, Liu J, Xiao Z, Siderovski DP, Du Q (2010) LGN regulates mitotic spindle orientation during epithelial morphogenesis. *J Cell Biol* 189: 275–288. <https://doi.org/10.1083/jcb.200910021> PMID: 20385777
10. Hao Y, Du Q, Chen X, Zheng Z, Balsbaugh JL, Maitra S, Shabanowitz J, Hunt DF, MacAra IG (2010) Par3 controls epithelial spindle orientation by aPKC-mediated phosphorylation of apical pins. *Curr Biol* 20: 1809–1818. <https://doi.org/10.1016/j.cub.2010.09.032> PMID: 20933426
11. McCaffrey LM, Macara IG (2011) Epithelial organization, cell polarity and tumorigenesis. *Trends Cell Biol* 21: 727–735. <https://doi.org/10.1016/j.tcb.2011.06.005> PMID: 21782440
12. Bellache Y, Radovic A, Woods DF, Hough CD, Parmentier ML, O’Kane CJ, Bryant PJ, Schweisguth F (2001) The Partner of Inscuteable/Discs-large complex is required to establish planar polarity during asymmetric cell division in *Drosophila*. *Cell* 106: 355–366. PMID: 11509184
13. Johnston CA, Hirono K, Prehoda KE, Doe CQ (2009) Identification of an Aurora-A/PinsLINKER/ Dlg Spindle Orientation Pathway using Induced Cell Polarity in S2 Cells. *Cell* 138: 1150–1163. <https://doi.org/10.1016/j.cell.2009.07.041> PMID: 19766567
14. Saadaoui M, Machicoane M, di Pietro F, Etoc F, Echard A, Morin X (2014) Dlg1 controls planar spindle orientation in the neuroepithelium through direct interaction with LGN. *J Cell Biol* 206: 707–717. <https://doi.org/10.1083/jcb.201405060> PMID: 25202028
15. Nakajima Y-I, Meyer EJ, Kroesen A, McKinney S a., Gibson MC (2013) Epithelial junctions maintain tissue architecture by directing planar spindle orientation. *Nature* 500: 1–5.
16. Navarro C, Nola S, Audebert S, Santoni M-J, Arsanto J-P, Ginestier C, Marchetto S, Jacquemier J, Isnardon D, Le Bivic A, et al. (2005) Junctional recruitment of mammalian Scribble relies on E-cadherin engagement. *Oncogene* 24: 4330–4339. <https://doi.org/10.1038/sj.onc.1208632> PMID: 15806148
17. Sottocornola R, Royer C, Vives V, Tordella L, Zhong S, Wang Y, Ratnayaka I, Shipman M, Cheung A, Gaston-Massuet C, et al. (2010) ASPP2 Binds Par-3 and Controls the Polarity and Proliferation of Neural Progenitors during CNS Development. *Dev Cell* 19: 126–137. <https://doi.org/10.1016/j.devcel.2010.06.003> PMID: 20619750
18. Lu B, Roegiers F, Jan LY, Jan YN (2001) Adherens junctions inhibit asymmetric division in the *Drosophila* epithelium. *Nature* 409: 522–525. <https://doi.org/10.1038/35054077> PMID: 11206549
19. Morais-de-Sá E, Sunkel C (2013) Adherens junctions determine the apical position of the midbody during follicular epithelial cell division. *EMBO Rep* 14: 696–703. <https://doi.org/10.1038/embor.2013.85> PMID: 23774295
20. Umbas R, Schalken J a, Aalders TW, Carter BS, Karthaus HFM, Schaafsma HE, Debruyne FMJ, Isaacs WB (1992) Expression of the cellular adhesion molecular E-cadherin is reduced or absent in high-grade prostate cancer. *Cancer Res* 52: 5104–5109. PMID: 1516067
21. Umbas R, Isaacs W, Bringuier P, Schaafsma H, Karthaus H, Oosterhof G, Debruyne F, Schalken J (1994) Decreased E-cadherin expression is associated with poor prognosis in patients with prostate cancer. *Cancer Res* 54: 3929–3934. PMID: 7518346
22. Graff JR, Herman JG, Lapidus RG, Chopra H, Xu R, Pitha PM, Davidson NE, Baylin SB, Jarrard DF, Isaacs WB (1995) E-Cadherin Expression Is Silenced by DNA Hypermethylation in Human Breast and Prostate Carcinomas. *Cancer Res* 55: 5195–5199. PMID: 7585573
23. Lechler T, Fuchs E (2005) Asymmetric cell divisions promote stratification and differentiation of mammalian skin. *Nature* 437: 275–280. <https://doi.org/10.1038/nature03922> PMID: 16094321
24. Toyoshima F, Nishida E (2007) Integrin-mediated adhesion orients the spindle parallel to the substratum in an EB1- and myosin X-dependent manner. *EMBO J* 26: 1487–1498. <https://doi.org/10.1038/sj.emboj.7601599> PMID: 17318179
25. Zimdahl B, Ito T, Blevins A, Bajaj J, Konuma T, Weeks J, Koechlein CS, Kwon HY, Arami O, Rizzieri D, et al. (2014) Lis1 regulates asymmetric division in hematopoietic stem cells and in leukemia. *Nat Genet* 46: 245–252. <https://doi.org/10.1038/ng.2889> PMID: 24487275
26. Poulson ND, Lechler T (2010) Robust control of mitotic spindle orientation in the developing epidermis. *J Cell Biol* 191: 915–922. <https://doi.org/10.1083/jcb.201008001> PMID: 21098114

27. Peyre E, Jaouen F, Saadaoui M, Haren L, Merdes A, Durbec P, Morin X (2011) A lateral belt of cortical LGN and NuMA guides mitotic spindle movements and planar division in neuroepithelial cells. *J Cell Biol* 193: 141–154. <https://doi.org/10.1083/jcb.201101039> PMID: 21444683
28. Roegiers F, Jan YN (2004) Asymmetric cell division. *Curr Opin Cell Biol* 16: 195–205. <https://doi.org/10.1016/j.ceb.2004.02.010> PMID: 15196564
29. Morin X, Jaouen F, Durbec P (2007) Control of planar divisions by the G-protein regulator LGN maintains progenitors in the chick neuroepithelium. *Nat Neurosci* 10: 1440–1448. <https://doi.org/10.1038/nn1984> PMID: 17934458
30. Siller KH, Doe CQ (2009) Spindle orientation during asymmetric cell division. *Nat Cell Biol* 11: 365–374. <https://doi.org/10.1038/ncb0409-365> PMID: 19337318
31. Eder AM, Sui X, Rosen DG, Nolden LK, Cheng KW, Lahad JP, Kango-Singh M, Lu KH, Warneke CL, Atkinson EN, et al. (2005) Atypical PKC ζ contributes to poor prognosis through loss of apical-basal polarity and cyclin E overexpression in ovarian cancer. *Proc Natl Acad Sci U S A* 102: 12519–12524. <https://doi.org/10.1073/pnas.0505641102> PMID: 16116079
32. Aranda V, Haire T, Nolan ME, Calarco JP, Rosenberg AZ, Fawcett JP, Pawson T, Muthuswamy SK (2006) Par6-aPKC uncouples ErbB2 induced disruption of polarized epithelial organization from proliferation control. *Nat Cell Biol* 8: 1235–1245. <https://doi.org/10.1038/ncb1485> PMID: 17060907
33. Nolan ME, Aranda V, Lee S, Lakshmi B, Basu S, Allred DC, Muthuswamy SK (2008) The polarity protein Par6 induces cell proliferation and is overexpressed in breast cancer. *Cancer Res* 68: 8201–8209. <https://doi.org/10.1158/0008-5472.CAN-07-6567> PMID: 18922891
34. McCaffrey LM, Montalbano J, Mihai C, Macara IG (2012) Loss of the Par3 Polarity Protein Promotes Breast Tumorigenesis and Metastasis. *Cancer Cell* 22: 601–614. <https://doi.org/10.1016/j.ccr.2012.10.003> PMID: 23153534
35. McCaffrey LM, Macara IG (2009) The Par3/aPKC interaction is essential for end bud remodeling and progenitor differentiation during mammary gland morphogenesis. *Genes Dev* 23: 1450–1460. <https://doi.org/10.1101/gad.1795909> PMID: 19528321
36. Qin Y, Capaldo C, Gumbiner BM, Macara IG (2005) The mammalian Scribble polarity protein regulates epithelial cell adhesion and migration through E-cadherin. *J Cell Biol* 171: 1061–1071. <https://doi.org/10.1083/jcb.200506094> PMID: 16344308
37. Bilder D, Perrimon N (2000) Localization of apical epithelial determinants by the basolateral PDZ protein Scribble. *Nature* 403: 676–680. <https://doi.org/10.1038/35001108> PMID: 10688207
38. Carvalho CA, Moreira S, Ventura G, Sunkel CE, Morais-De-Sá E (2015) Aurora a triggers Lgl cortical release during symmetric division to control planar spindle orientation. *Curr Biol* 25: 53–60. <https://doi.org/10.1016/j.cub.2014.10.053> PMID: 25484294
39. Bergstralh DT, Lovegrove HE, St Johnston D (2013) Discs large links spindle orientation to apical-basal polarity in drosophila epithelia. *Curr Biol* 23: 1707–1712. <https://doi.org/10.1016/j.cub.2013.07.017> PMID: 23891112
40. Bianchini JM, Siemers KA, Cohen DJ, Gloerich M, Nelson WJ (2017) adhesion by the E-cadherin / LGN complex. *Nat Commun* 8: 1–11. <https://doi.org/10.1038/s41467-016-0009-6>
41. Gloerich M, Bianchini JM, Siemers KA, Cohen DJ, Nelson WJ (2017) Cell division orientation is coupled to cell-cell adhesion by the E-cadherin/LGN complex. *Nat Commun* 8: 1–11. <https://doi.org/10.1038/s41467-016-0009-6>
42. Xue B, Krishnamurthy K, Allred DC, Muthuswamy SK (2012) Loss of Par3 promotes breast cancer metastasis by compromising cell-cell cohesion. *Nat Cell Biol* 15: 1–14.
43. Feigin ME, Akshinthala SD, Araki K, Rosenberg AZ, Muthuswamy LB, Martin B, Lehmann BD, Berman HK, Pietenpol JA, Cardiff RD, et al. (2014) Mislocalization of the cell polarity protein scribble promotes mammary tumorigenesis and is associated with basal breast cancer. *Cancer Res* 74: 3180–3194. <https://doi.org/10.1158/0008-5472.CAN-13-3415> PMID: 24662921
44. Pearson HB, Perez-Mancera PA, Dow LE, Ryan A, Tennstedt P, Bogani D, Elsum I, Greenfield A, Tuveson DA, Simon R, et al. (2011) SCRIB expression is deregulated in human prostate cancer, and its deficiency in mice promotes prostate neoplasia. *J Clin Invest* 121: 4257–4267. <https://doi.org/10.1172/JCI58509> PMID: 21965329
45. Becker KF, Atkinson MJ, Reich U, Becker I, Nekarda H, Siewert JR (1994) E-Cadherin Gene Mutations Provide Clues to Diffuse Type Gastric Carcinomas. *Cancer Res* 54: 3845–3852. PMID: 8033105
46. Ceteci F, Ceteci S, Karreman C, Kramer BW, Asan E, Götz R, Rapp UR (2007) Disruption of Tumor Cell Adhesion Promotes Angiogenic Switch and Progression to Micrometastasis in RAF-Driven Murine Lung Cancer. *Cancer Cell* 12: 145–159. <https://doi.org/10.1016/j.ccr.2007.06.014> PMID: 17692806
47. Derksen PWB, Liu X, Saridin F, van der Gulden H, Zevenhoven J, Evers B, van Beijnum JR, Griffioen AW, Vink J, Krimpenfort P, et al. (2006) Somatic inactivation of E-cadherin and p53 in mice leads to

metastatic lobular mammary carcinoma through induction of anoikis resistance and angiogenesis. *Cancer Cell* 10: 437–449. <https://doi.org/10.1016/j.ccr.2006.09.013> PMID: 17097565

48. Toivanen R, Mohan A, Shen MM (2016) Basal Progenitors Contribute to Repair of the Prostate Epithelium Following Induced Luminal Anoikis. *Stem Cell Reports* 6: 660–667. <https://doi.org/10.1016/j.stemcr.2016.03.007> PMID: 27117783
49. Zhang K, Zhao H, Ji Z, Zhang C, Zhou P, Wang L, Chen Q, Wang J, Zhang P, Chen Z, et al. (2016) Shp2 promotes metastasis of prostate cancer by attenuating the PAR3 / PAR6 / aPKC polarity protein complex and enhancing epithelial-to-mesenchymal transition. 1271–1282. <https://doi.org/10.1038/onc.2015.184> PMID: 26050620